# Combined Receptor and Ligand-Based Approach to the Universal Pharmacophore Model Development for Studies of Drug Blockade to the hERG1 Pore Domain

Serdar Durdagi,[†] Henry J. Duff,[*,‡] and Sergei Yu. Noskov[*,†]

[†]Department of Biological Sciences, University of Calgary, Institute for Biocomplexity and Informatics Calgary, Alberta, Canada
[‡]Faculty of Medicine, University of Calgary, Libin Cardiovascular Institute of Alberta, Calgary, Alberta, Canada

S *Supporting Information*

ABSTRACT: Long QT syndrome, LQTS, results in serious cardiovascular disorders, such as tachyarrhythmia and sudden cardiac death. A promiscuous binding of different drugs to the intracavitary binding site in the pore domain (PD) of human ether-a-go-go related gene (hERG) channels leads to a similar dysfunction, known as a drug-induced LQTS. Therefore, an assessment of the blocking ability for potent drugs is of great pragmatic value for molecular pharmacology and medicinal chemistry of hERGs. Thus, we attempted to create an in silico model aimed at blinded drug screening for their blocking ability to the hERG1 PD. Two distinct approaches to the drug blockage, ligand-based QSAR and receptor-based molecular

docking methods, are combined for development of a universal pharmacophore model, which provides rapid assessment of drug blocking ability to the hERG1 channel. The best 3D-QSAR model (AAADR.7) from PHASE modeling was selected from a pool consisting of 44 initial candidates. The constructed model using 31 hERG blockers was validated with 9 test set compounds. The resulting model correctly predicted the pIC_{50} values of test set compounds as true unknowns. To further evaluate the pharmacophore model, 14 hERG blockers with diverse hERG blocking potencies were selected from literature and they were used as additional external blind test sets. The resulting average deviation between in vitro and predicted pIC_{50} values of external test set blockers is found as 0.29 suggesting that the model is able to accurately predict the pIC_{50} values as true unknowns. These pharmacophore models were merged with a previously developed atomistic receptor model for the hERG1 PD and exhibited a high consistency between ligand-based and receptor-based models. Therefore, the developed 3D-QSAR model provides a predictive tool for profiling candidate compounds before their synthesis. This model also indicated the key functional groups determining a high-affinity blockade of the hERG1 channel. To cross-validate consistency between the constructed hERG1 pore domain and the pharmacophore models, we performed docking studies using the homology model of hERG1. To understand how polar or nonpolar moieties of inhibitors stimulate channel inhibition, critical amino acid replacement (i.e., T623, S624, S649, Y652 and F656) at the hERG cavity was examined by in silico mutagenesis. The average docking score differences between wild type and mutated hERG channels was found to have the following order: F656A > Y652A > S624A > T623A > S649A. These results are in agreement with experimental data.
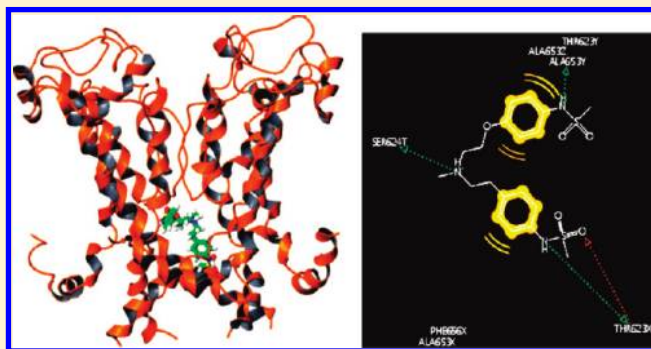
■ INTRODUCTION

The human ether-a-go-go related gene 1 (hERG1) K ion channel (also referred to as KCNH2 or Kv11.1) is a key element for the rapid component of the delayed rectified potassium currents (IKr) in cardiac myocytes, required for the normal repolarization phase of the cardiac action potential.[1−3] Loss of function mutations in hERG1 cause increased duration of ventricular repolarization, which leads to prolongation of the time interval between Q and T waves of the body surface electrocardiogram (long QT syndrome-LQTS).[3−5] The majority of hERG mutations causing LQTS are located in trans-membrane (TM) domains such as the voltage-sensing (VS) helical bundle comprising
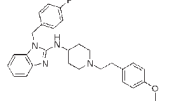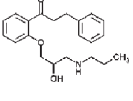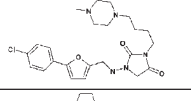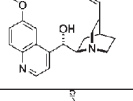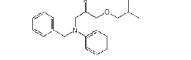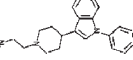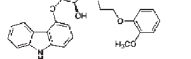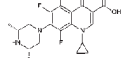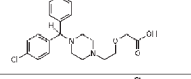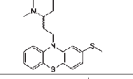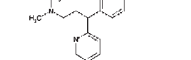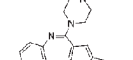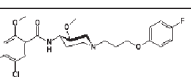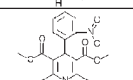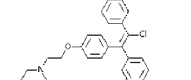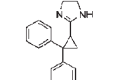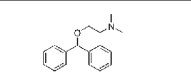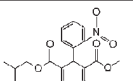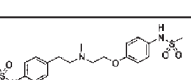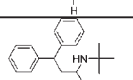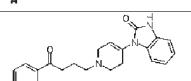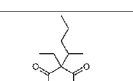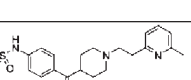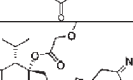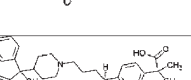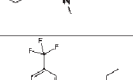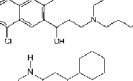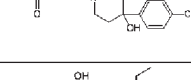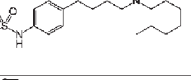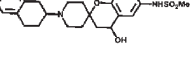
helices S1−S4 and the pore-domain (PD) formed by S5-pore-S6 helices.[4−10] LQTS leads to serious cardiovascular disorders, such as tachyarrhythmia and sudden cardiac death. Therefore, an accurate understanding of the molecular basis of the blockade of the hERG channel is essential to facilitate the design of safe drugs.[11−13]

Diverse types of organic compounds used both in common cardiac and noncardiac medications, such as antibiotics, antihistamines, and antibacterial, can reduce the repolarizing current
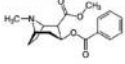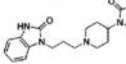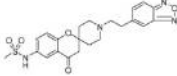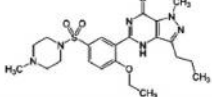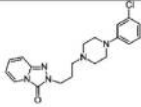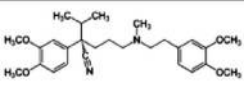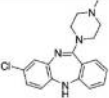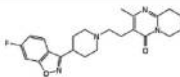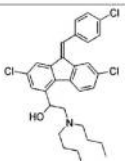
Table 1. Thirty-One Ligands with Diverse Activities at the Target Were Used to Construct the Pharmacophore Model[a]

Training set Comp. No.	Name	Structure	Activity pIC$_{50}$	Predicted pIC$_{50}$	Confor- mations	Comp. No.	Name	Structure	Activity pIC$_{50}$	Predicted pIC$_{50}$	Confor- mations
1	Astemizole		9.05	9.09	89	18	Propafenone		5.67	5.62	41
2	Azimilide		6.25	6.31	172	19	Quinidine		6.49	6.37	14
3	Bepridil		6.26	-	86	20	Sertindole		8.52	-	59
4	Carvedilol		4.98	4.97	73	21	Sparfloxacin		4.74	4.78	14
5	Cetirizine		4.52	-	104	22	Thioridazine		7.48	-	49
6	Chlorfeniramine		4.68	-	28	23	Olanzapine		6.70	6.61	2
7	Cisapride		8.19	8.25	166	24	Nifedipine		5.22	5.37	8
8	Clomiphene		6.74	-	123	25	Cibenzoline		5.85	-	6
9	Diphenydramine		4.57	-	37	26	Nisoldipine		5.52	5.51	82
10	Dofetilide		8.02	7.98	163	27	Terodiline		6.46	-	7
11	Droperidol		7.49	7.52	87	28	Pentobarbital		5.21	5.11	3
12	E4031		8.14	8.18	126	29	Mibefradil		6.10	6.03	49
13	Fexofenadine		4.67	-	87	30	Halofantrine		7.47	-	41
14	Haloperidol		7.73	7.65	90	31	Perhexilin		5.11	-	11
15	Ibutilide		8.00	7.93	165						
16	MK-499		7.49	7.45	18						
17	Pimozide		7.74	-	73						

[a] The table shows number of conformations used for the construction of the pharmacophore model, their structures, and experimental and predicted pIC$_{50}$ values. PHASE skips the prediction of pIC$_{50}$ values of compounds that have poor alignment with the pharmacophore hypothesis.

Table 2. Nine Ligands Were Used to Validate the Constructed Pharmacophore Model[a]

Test set Comp. No.	Name	Structure	Activity pIC$_{50}$	Predicted pIC$_{50}$	Confor-mations	Comp. No.	Name	Structure	Activity pIC$_{50}$	Predicted pIC$_{50}$	Confor-mations
T1	Cocaine		5.36	4.92	6	T6	Domperidone		6.79	6.81	85
T2	L691121		8.10	8.00	94	T7	Sildenafil		5.48	5.57	104
T3	Trazodone		5.54	5.91	96	T8	Verapamil		6.84	6.42	85
T4	Clozapine		6.72	6.07	2	T9	Risperidone		6.82	7.14	21
T5	Lumefantrine		4.36	4.48	41						

[a] These structures represent the full spectra of features found in active and inactive hERG blockers. The table represents structures of test set ligands, their number of conformations, experimental and predicted pIC$_{50}$ values.

IKr (i.e., with binding to the central cavity of the pore domain of hERG1) and lead to ventricular arrhythmia.[7,13,14] Therefore, several approved drugs (i.e., terfenadine, cisapride, astemizole, and grepafloxin) have been withdrawn from the market, whereas several drugs, such as thioridazine, haloperidol, sertindole, and pimozide, are restricted in their use because of their effects on QT interval prolongation.[15,16]

The recommended in vitro drug screening process includes traditional patch clamp techniques, radiolabeled drug binding assays, 86RB-flux assays, and high-throughput cell-based fluorescent dyes and stably transfected hERG1 ion channels from Chinese hamster ovary (CHO) cells.[17] Although elaborate nonclinical tests display a reasonable sensitivity and establish safety standards for novel therapeutics, the screening of all of potential candidates remains very time-consuming and thus increases the final cost of drug design. Molecular modeling techniques can possibly assist in screening drug candidates for their blocking ability to the hERG1. In this study, an evaluation of the 3D quantitative structure–activity relationships (QSAR)/PHASE algorithm has been performed for diverse set of hERG blockers. Several studies report the utilization of QSAR methods for studying drug binding to K-channels,[18] including hERG1 blockers.[19−23] The main idea of QSAR methods is to utilize a general pharmacophore model that can combine information of key functional groups of the ligand and available experimental information on binding for a data set of ligands. A major weakness of approaches based on QSAR is in the alignment and low-resolution of the molecules, as well as a lack of information on protein-drug complexes. A fine-grained conformational sampling for each ligand in the data set, such as the one that PHASE uses, minimizes the weakness of the ligand-based approach.

In parallel, many research groups have been working on receptor-based models of hERG-drug interactions based on molecular docking and molecular dynamics (MD) simulations studies. A number of atomistic receptor models have been

developed by different groups, and it was observed that available crystal structures for potassium channels provide an adequate platform for studies of drug blocking of the pore domain of the hERG1 channel.[24−30] Molecular modeling studies may therefore provide atomistic details about interactions governing high-affinity drug binding to the intracellular cavity of the hERG1 channel. Many drugs, however, block hERG1 channels in a voltage-dependent manner targeting only a particular state of the channel (e.g., open state, inactivated state). Therefore, an accurate atomistic approach to the binding affinities for a panel of known or designed blockers must either (a) explicitly consider all states of the protein or (b) utilize empirical constraints. Whereas evaluating drug binding for all possible conformational states of the channel is a robust and preferred solution to the problem, it is computationally unfeasible. The combination of atomistic models and QSAR models may provide a readily available combination for building a pharmacophore model for hERG1 blockers, which includes both receptor and ligand information explicitly. Although impressive progress has been made on structural and QSAR modeling of hERG1 channel blockers, there is no reported study to date combining and cross-validating ligand-based (QSAR) and receptor-based (atomistic) models. To combine the advantages of both approaches, which are very different in nature but similar in aims, we first performed 3D-QSAR/PHASE modeling.[31] This algorithm utilizes fine-grained conformational sampling and a range of scoring techniques to identify common pharmacophore hypotheses, which convey characteristics of 3D chemical structures that are purported to be critical for binding. Next, we evaluated the consistency between the constructed 3D-QSAR and receptor-based hERG-drug models extracted from docking studies on a broad panel of compounds with three different docking algorithms. Finally, we ranked the importance of a particular amino acid in the hERG1 inner cavity for drug stabilization with *in-silico* alanine scanning. This ranking helps to probe an intrinsic relationship between

hydrophobic or polar moieties of blockers and molecular structure of the inner cavity, whereby providing a general tool to understand key determinants in the high-affinity blockade of the hERG1. Combination of these modeling techniques allows the evaluation of the consistency between the two approaches and led to the development of a universal pharmacophore model (available upon request from www.noskovlab.com).

■ COMPUTATIONAL METHODS

Generation of 3D Structures and their Conformers for Training and Test Set Ligands. Molecular structures of all ligands used to create pharmacophore models are shown in the Table 1. Ligands that used to validate the model were shown in the Table 2. Prior to the modeling, all drugs were built and minimized with the Maestro (v.8.5.207) module of the Schrödinger molecular modeling package.[32] The Polak–Ribiere conjugate gradient (PRCG) method with a 0.001 kcal/mol Å convergence threshold was used for the geometry optimization calculations.

These structures were then incorporated into the LigPrep (v.2.2) module of Schrödinger.[32] The protonation state for all ionizable groups was set at neutral pH = 7. A conformational search was performed with the Monte Carlo Multiple Minimum (MCMM) method (with the 'enhanced' torsion sampling option) to derive representative conformers for each ligand in the training and test sets.[31] Input structures were minimized and modified by random changes in torsion angles and molecular position. The created conformers were examined if already found by the MCMM procedure. This step allows a new search to be initialized from the output of a previous search, by using the output file of the old search as input for the new one. Only unique structures (based on given threshold input criterias) will be retained during the conformational search. In this study, the maximum number of steps was set to 1000 with 100 steps per every rotatable bond. The energy window for saving the structures was set to 21.0 kJ/mol. An RMSD cutoff of 0.5 Å was used to eliminate redundant conformers. The number of conformers for each ligand used in this study is shown in Tables 1 and 2.

Construction of 3D QSAR Models. The 3D QSAR study was carried out with the PHASE (v.3.0) program of the Schrodinger molecular modeling package.[31] The pIC_{50} values were used instead of IC_{50} values for each ligand in the training and test sets by calculating $-\log[IC_{50}]$. We used a common notation for the pharmacophore site, where every structure in the training and test sets is represented by a 3D-contour mapping key chemical features favoring complex receptor–ligand complex formation. Pharmacophore sites were derived for the different conformations. The specific interactions between a target and a ligand depend on a structural complimentarity between functional groups presented in the ligand and coordinating residues from the binding pocket. PHASE classifies these chemical features as hydrogen bond acceptors (labeled as A), hydrogen bond donors (labeled as D), hydrophobic groups (labeled as H), negatively charged groups (labeled as N), positively charged groups (labeled as P), and aromatic rings (labeled as R).[31] A hydrogen-bond acceptor site is determined as surface-accessible atoms, which may also carry lone pairs. A "vector attribute" was assigned to each idealized hydrogen bond axis according to the hybridization of the acceptor atom.[31] A hydrogen-bond donor site is centered on a polar hydrogen atom and a single vector feature is directed along with the hydrogen bond axis.

Rings, isopropyl groups, *t*-butyl groups, various halogenated moieties and chains as long as four carbons are treated as a single hydrophobic site.[31] Chains of five or more carbons are broken into smaller fragments (5 (2 + 3); 6 (3 + 3); 7 (3 + 4), etc.), and each of the fragments is designated as a separate hydrophobic site.

PHASE uses the most active compounds (high affinity) in the training set to build the pharmacophores. To define a common pharmacophore or hypothesis, PHASE employs an analysis of *k*-point pharmacophores derived from the conformational sets of active compounds and then identifies all spatial arrangements with pharmacophore features that are shared by those molecules.[31] In this study, we set a pIC_{50} threshold for the selection of active and inactive ligands ($IC_{50} > 10\,\mu M$, $pIC_{50} < 5$) considered as inactive (i.e., weak blocker) and $IC_{50} < 50$ nM, $pIC_{50} > 7.3$ considered as active ligands (i.e., strong blockers). Thus, a common pharmacophore must match a minimum required number of active ligands, which was set as 5 in this study. Pharmacophores from different conformations of all five active ligands in the training set were analyzed, and those conformations with identical sets of five pharmacophore sites that were similarly spatially arranged were clustered and scored.[31] (The details of scoring functions can be found in the Supporting Material.) All parameters used during the 3D QSAR model construction had default values except for the maximum number of partial least-squares (PLS) factors (i.e., 3), the 3D QSAR model type (i.e., atom-based), and the percent of ligand assigned to the training and test sets (i.e., 77% and 23%, respectively). The test set ligands (see Table 2) were selected by the program from the data set, and they were sufficiently diverse in structure and activity ($>5 \times 10^3$-fold IC_{50} range). PLS factor 2 was used for the construction of contour plots.

Molecular Docking. Three different docking algorithms (Glide/Induced Fit Docking (IFD),[33] GOLD,[34] and FlexX[35]) were used to study drug docking to the previously developed receptor model.[30] Details of the methodologies of these algorithms are provided below:

Glide/IFD. The Glide-XP (extra precision) (v.5.0)[33] combined with IFD was used for the docking calculations. IFD uses the Glide docking program to account for the ligand flexibility and the refinement module. Prime algorithm implemented in Glide to account for the flexibility of the receptor.[36] Residues within 10.0 Å of the ligand poses were minimized to form suitable conformations of poses at the active site of the receptor. Glide redocking was performed for each protein–ligand complex. In docking simulations, inner and outer cavity radii were selected as 20 and 30 Å, respectively.

GOLD. GOLD (v.4.1.1)[34] was used under a Linux operating system. The binding interactions are derived using a genetic algorithm. Block functions of two docking scores (GOLD fitness score and ChemScore) with default values were used. The active site was constructed with a 20 Å radial cavity from the origin of the receptor inner cavity. Partial flexibility of the receptor was gained with 10 amino acid residues at the active site. Side chains of these amino acid residues were selected as flexible rotamers with 10° increments with scanning of 360°. The default generic algorithm parameters were used.

FlexX. FlexX (v.4.0)[35] from BioSolveIT was used. A radius cavity of 20 Å from the origin of receptor's inner cavity was used.

Analysis of Top Docking Poses. The LigandScout program[37] was used to investigate essential residues for their high-affinity blocking potency and their interactions with blockers

Table 3. (a) Statistical Parameter Values for the Best 3D QSAR Model AAADR.7 and (b) Derived Scores for the Constructed Model.

(a)								
PLS factor	SD	R^2	F	P	RMSE	Q^2	R-Pearson	reference ligand
1	0.56	0.82	91.8	6.46×10^{-9}	0.215	0.85	0.97	E4031
2	0.19	0.98	447.0	1.05×10^{-16}	0.236	0.82	0.92	E4031
3	0.08	0.99	2058.4	5.21×10^{-23}	0.281	0.74	0.88	E4031

(b)						
survival active	survival inactive	site	vector	volume	selectivity	matches
3.090	2.639	0.780	0.939	0.374	1.237	5
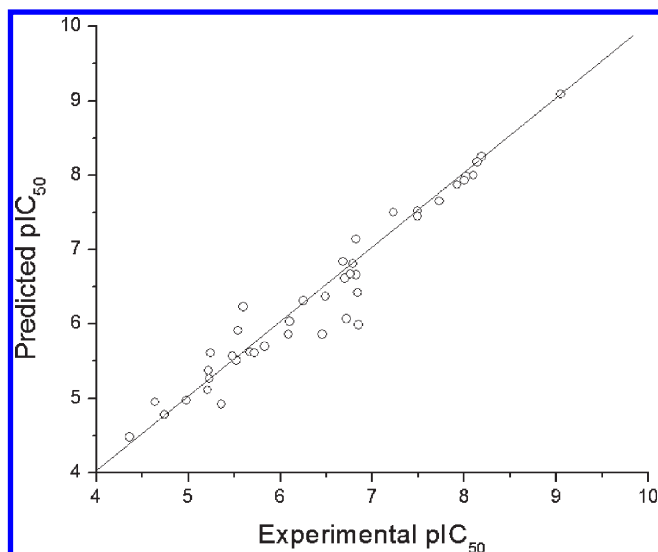
Figure 1. Plot of experimental and predicted values of binding affinities (given as pIC$_{50}$) of hERG1 inhibitors in the training set and test set (including external test set) (see also Tables 1 and 2 and Supporting Information Table S2).

from docking complexes. The interaction cutoff threshold of the pdb interpretation settings was set to 12 Å. This threshold defines a sphere (in Å) around the ligand. All atoms of the protein, which are enclosed inside the sphere, are considered as possible interactions. All of the remaining settings were maintained as the default.

■ RESULTS

Pharmacophore Model Design. Forty hERG1 inhibitors with a broad range of inhibition (0.89 to 43700 nM) were selected from literature.[38,19] Pharmacophore model was constructed with 31 hERG blockers with diverse binding affinities (Table 1) and rest of the 9 compounds were used in the detailed validation and testing of the constructed model (Table 2). The 3D-QSAR studies were performed using the PHASE program of Schrodinger molecular modeling package which derived 44 pharmacophore models. After all the 44 3D-QSAR models had been built, statistical analysis is performed for each model and, they were used to predict pIC$_{50}$ values of hERG blockers from the training and test sets. Then, from the comparison between experimental and predicted pIC$_{50}$, statistical results were derived to describe how efficient each 3D-QSAR model is for predicting the pIC$_{50}$ values of hERG blockers. While R^2, SD, F, and P results

were used to evaluate the training set predictions; Q^2, RMSE, and Pearson R values were used to evaluate the test set predictions. Finally these results were considered to rank the created 44 pharmacophore models (i.e., highest R^2, Q^2, and Pearson R and lowest RMSE, SD, and P values), and one of them (AAADR.7) were used for further analysis. Statistical parameter values for the best 3D QSAR model (AAADR.7) out of the 44 constructed models are shown in Table 3. For comparison reasons, derived statistical results of all 44 3D-QSAR models were also represented (Table S1 of the Supporting Information). Experimental and corresponding predicted pIC$_{50}$ values of training and test sets hERG1 inhibitors are collected in Tables 1 and 2, respectively, and plotted in Figure 1 (it includes also activity profiles of external test set compounds). A very high correlation coefficient ($R^2 = 0.98$) between experimental and predicted binding affinity values of the training set ligands indicates the model reliability comparable to prior QSAR studies.[19−23] The predictive ability of the model has been blind-tested with separate 9 test set compounds, and it was able to accurately predict the pIC$_{50}$ values as true unknowns.

In Figures 2A and B, the results of the analysis of the AAADR.7 model on the functional importance of different chemical groups are shown as contour maps for strong and weak blockers of the hERG channel. Although the importance of hydrophobic matching in the hERG1 blockade was emphasized in many studies, analysis of the hydrogen-bonding pattern may provide a very clear distinction between two limiting cases of weak and tight block. In the case of a strong blocker, the preservation of the hydrogen-bonding ability in the structure was complemented by matching the hydrophobic zone and provides a high-affinity block or "active pharmacophore". An example of an almost exact match between H-bond donor contour maps and H-bond acceptors in one of the strong blockers, E4031, is shown in Figure 2A, left. The green-colored H-bond donor favorable contours overlap with the amine group (labeled as D in the figure); H-bond acceptor groups (i.e., carbonyl and sulfone, labeled as A in the figure) match with the brown colored H-bond donor (unfavorable) contours. For the weak blocker carvedilol, green colored H-bond donor favorable fields in the pharmacophore model do not overlap with the donor groups of the ligand (i.e., −NH moiety of carbazol group, labeled as D in Figure 2A, right, match with the brown H-bond donor (unfavorable fields) in the actual drug).

Results of the hydrophobicity analysis are shown in Figure 2B for two strong hERG blockers, dofetilide (top-left in the figure) and L691121 (top-right in the figure) and two weak blockers, sparfloxacin (bottom-left in the figure) and carvedilol (bottom-right in the figure), respectively. In accordance with previous
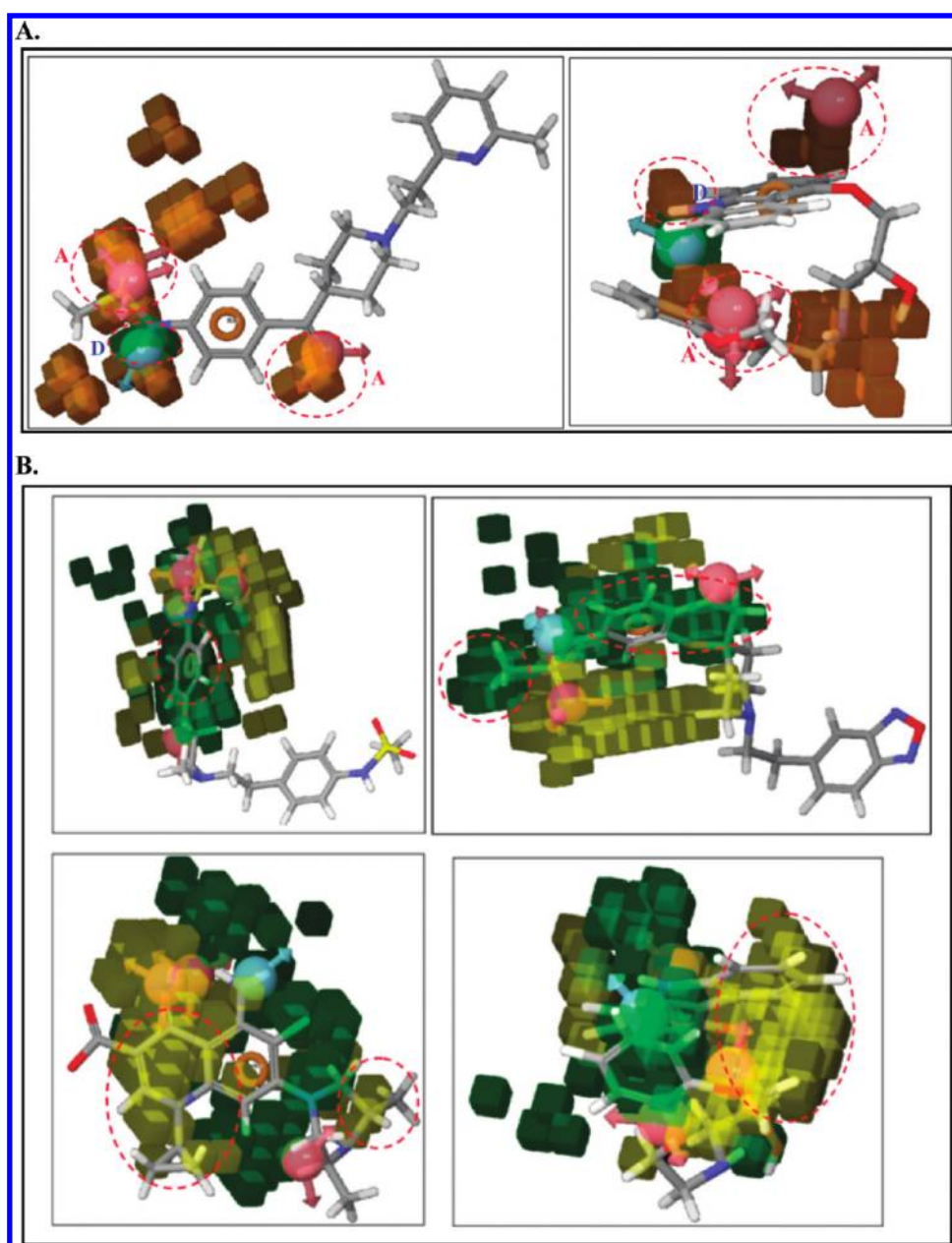
Figure 2. A. (top) The visualization of H-bond donor features of AAADR.7 model in the context of the high affinity hERG blocker E4031 (pIC$_{50}$ = 8.14) (left) and weak blocker carvedilol (pIC$_{50}$ = 4.98) (right). Green fields show H-bond donor favorable and brown colored fields represent H-bond donor disfavorable areas. These areas fit perfectly with the corresponding atoms in strong blocker E4031, however in weak blocker carvedilol green colored H-bond donor favorable fields do not fit with the donor atoms (i.e., −NH (labeled with D in carvedilol) is in the brown field of disfavorable areas). (A and D labels in figures represent hydrogen-bond acceptor and hydrogen-bond donor pharmacophores, respectively). B. (bottom) The visualization of hydrophobic features of AAADR.7 model in the context of the high affinity blockers dofetilide (pIC$_{50}$ = 8.02) (top-left) and L691121 (pIC$_{50}$ = 8.10) (top-right) and weak blockers sparfloxacin (pIC$_{50}$ = 4.74) (bottom-left) and carvedilol (pIC$_{50}$ = 4.98) (bottom-right). Green fields show hydrophobic favorable, and brown fields represent hydrophobic disfavorable areas. These areas fit perfectly with the corresponding atoms in high affinity ligands dofetilide and L691121; however in inactive compounds, brown hydrophobic feature disfavorable fields fit with the nonpolar parts of compounds.

studies, hydrophobic features of the ideal pharmacophore overlap nicely with the matching functionality in high affinity ligands dofetilide and L691121 (i.e., green hydrophobic feature favorable contours match perfectly with corresponding aromatic rings and alkyl moiety of sulfone groups in dofetilide and L691121 in Figure 2B, top), but in weak blockers brown colored hydrophobic feature unfavorable fields fit with the nonpolar parts of compounds (i.e., cyclopropylpyridine part of sparfloxacin and aromatic ring moiety of carbazole in Figure 2B, bottom). Thus,

derived contour maps based on predicted regression equation coefficients are capable of differentiation between strong and weak hERG blockers. This leads to a conclusion that even a very promiscuous cavity such as hERG1 dictates a conservation of chemical features in the blocker, required for a high-affinity block. These features are not reducible to a hydrophobic matching alone, but indicate the requirement of complimentarity in hydrophobicity, hydrogen bonding/polarity and its aromaticity of the ideal blocker.

Validation of the Model. To blindly validate the constructed 3D-QSAR model, nine compounds (**T1**–**T9** in Table 2) were selected. The validation set created by PHASE includes compounds representing all categories of activity of the data set, that is, inactive and active compounds comprising all the structural features that important for the binding activity. Their in vitro pIC_{50} values range between 4.36 and 8.10 and their biological activities were predicted from the PLS equations (Table 2). The resulting average deviation between actual and predicted pIC_{50} values of test set compounds (Table 2) is found to be around 0.28, indicating high accuracy of the developed model. To further evaluate the predictive power and validate the constructed model, additional 14 known hERG blockers with diverse hERG blocking affinities (pIC_{50} values range between 4.64 and 7.92) that do not belong to the training set were selected from the literature and used as external test set compounds (see Supporting Information Table S2). Their experimental pIC_{50} values at the hERG1 target were predicted by the constructed model. The constructed model predicted correctly the pIC_{50} values of % 100 of external test set compounds within 1.0 logarithmic unit (this value is found as % 79 within 0.5 logarithmic unit). The average deviation of in vitro and predicted pIC_{50} values of external test compounds (Supporting Information Table S2) was found as 0.29 suggesting that the model is able to accurately predict the pIC_{50} values as true unknowns for the estimation of affinities of novel compounds prior to their synthesis.

Importantly, the constructed model is able to differentiate the "active" and "inactive" ligands. Such a model may be subsequently used to rank ligands for their hERG blocking affinities. A high selectivity of the AAADR.7 model (1.237, see Table 3) was found. Because the selectivity is determined on a logarithmic scale, 1.237 selectivity value means 1 in ∼17 molecules would be expected to match the hypothesis. Higher selectivity is desirable because it indicates that the hypothesis is more likely to be unique to the active set ligands.

Combining Ligand-Based Model with Receptor Based Model. To test the stability and performance of the ligand-based virtual hERG1 model, we merged it with an atomistic model of the hERG1 pore domain developed previously.[30] (Supporting Information Figure S1). The atomistic model for the pore domain used in the study represents the open state of the channel and this model was validated with experimental studies and provides a reasonable background for studies of drug block to hERG1.[30,39] The hERG blockers shown in Tables 1 and 2 were docked to the IC cavity of the receptor using three different programs: GOLD, Glide/IFD and FlexX docking programs. Binding scores derived from the docking studies were compared with the corresponding in vitro binding energies (binding energies were converted from in vitro binding affinities of inhibitors using $\Delta G = -RT \ln IC_{50}$, $T = 300$ K, $R = 8.314$ J/mol K). The correlation coefficient (r^2) between experimental binding energies and docking scores was found to be 0.61, 0.54, and 0.57 for the GOLD, Glide/IFD, and FlexX docking programs, respectively, which is comparable to previous studies (Supporting Information Figure S2).

The key residues involved in the drug stabilization were identified for a number of blockers from Tables 1 and 2. The locations of the amino acids contributing the most to the blocker stabilization in the intracellular (IC) cavity of the hERG1 match well with pharmacophores derived from the ligand-based model. Figure 3 shows the top binding docking poses of one of the most studied high-affinity hERG blockers, dofetilide (compound **10** in Table 1) in the hERG1 cavity. Critical residues necessary for the high-affinity blocking potency, and their interactions with the blocker were generated from these docking poses by LigandScout software[37] (Figure 3) (top docking modes (i.e., coordinate files of ligand–receptor complexes) were used as input). Red and green vectors indicate hydrogen bond acceptors and donors, respectively; yellow curved lines indicate hydrophobic interactions; and red and blue lines indicate negative and positive ionizable areas, respectively. Whereas hydrophobic interactions of Y652, F656, A653, and T623 have been observed for the top docking poses of dofetilide, electrostatic interactions have been observed for L622, T623, S624, and A653.

Top docking poses of reference ligand (E4031 in AAADR.7 hypothesis) binding poses produced by the three docking softwares (FlexX, GOLD and Glide/IFD) are superimposed with the conformation of E4031 in the AAADR.7 hypothesis (Supporting Information Figure S3). RMSDs of these conformations of E4031 produced by docking softwares and conformation of E4031 in the AAADR.7 hypothesis are found as 1.16 (conformation produced by FlexX), 1.38 (conformation produced by Glide/IFD), and 1.49 (conformation produced by GOLD) showing the consistency between ligand-based and receptor-based models.

To analyze contributions of polar and nonpolar protein moieties to high-affinity blockade, in silico single-point alanine scanning mutagenesis was performed guided by available experimental information.[19,40] The following mutated ion channels T623A, S624A, S649A, Y652A, and F656A were used in the protein preparation module of Schrödinger molecular modeling package and minimized with the RMSD threshold cutoff of 0.30 Å. The inhibitors in Tables 1 and 2 were docked to the prepared mutated ion channels, and docking scores were compared with corresponding docking scores at wild hERG1. The average docking score differences between wild type and mutated hERG channels was found to have the following order: F656A (1.93) > Y652A (0.84) > S624A (0.79) > T623A (0.77) > S649A (0.49) (numbers in parentheses showing the average differences of binding scores between wild and mutated hERG channels, in kcal/mol).

■ DISCUSSION

Understanding the complimentarity between the drug and the receptor is required to accurately predict the blocking properties of a new compound. The result of the QSAR analysis corresponds to a regression equation with thousands of coefficients, and a direct interpretation of the corresponding equation based on its coefficients is not always possible. The common consensus is to visualize the results is by the generation of contour maps representing favorable and unfavorable steric fields around the molecules, as well as electronegative and electropositive substituents in certain positions.[41] Generally speaking, contour maps are not considered to be equivalent to the corresponding binding pocket of the target protein. However, if the conformation of the ligand used in the model resembles its binding conformer, then the steric and electrostatic coefficient contours may correspond to some extent to the steric and electrostatic environments of the binding site.[42] Therefore, it is beneficiary to directly compare matching between predictions of QSAR models and atomistic docking. Below, we summarize what is known from previous studies and what has been found by a combination of QSAR and atomistic models. The challenge, however, is to merge two different approaches to the problem and to produce a pharmacophore model having all characteristic features of known
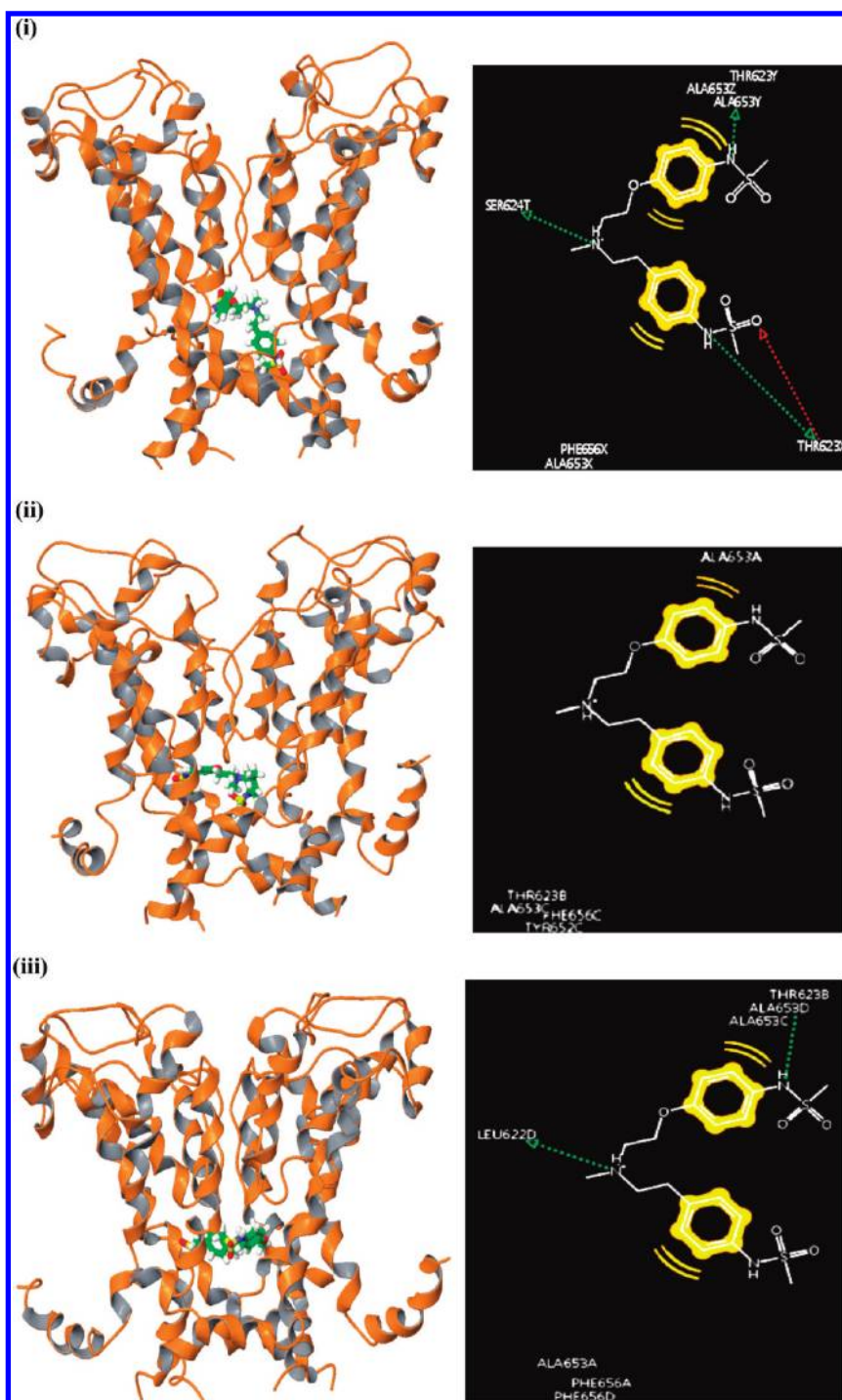
Figure 3. (left) Top binding poses of dofetilide at hERG1 by (i) FlexX, (ii) GOLD, and (iii) Glide/IFD docking programs. (right) Pharmacophore interactions of dofetilide (compound **11** at Table 1) with hERG1 amino acid residues. Input coordinates used from the top binding poses of dofetilide at hERG1 by (i) FlexX, (ii) GOLD, and (iii) Glide/IFD docking programs. Red and green vectors indicate hydrogen bond acceptors and donors, respectively; yellow curved lines indicate hydrophobic interactions, red and blue lines indicate negative and positive ionizable areas, respectively. (Letters after residue numbers indicate four chains at hERG1).

high-affinity blockers and yet complementing the unique organization of the intracellular (IC)-cavity (blockers binding pocket) in hERGs.

Many previous studies are highlighted the importance of terminal methylsulfonamide groups at hERG blockage.[43] For example a simple change of methylsulfonamide in compound *m* to the ethylsulfonamide in compound *n* resulted in 4-fold

decrease in hERG IC$_{50}$ (Supporting Information Figure S4). Similar study has been performed for benzylpiperidines, the isopropylsulfonamide in compound *p* showed a 240-fold reduced hERG IC$_{50}$ upon comparison with the methylsulfonamide derivative, compound *r* (Supporting Information Figure S4). In these examples, the reduction of hERG IC$_{50}$ values may be attributed to the specific structural changes in the periphery of

Figure 4. Alignment of AAADR.7 pharmacophores with reference compound E4031. Distances between pharmacophores were also shown in the figure.

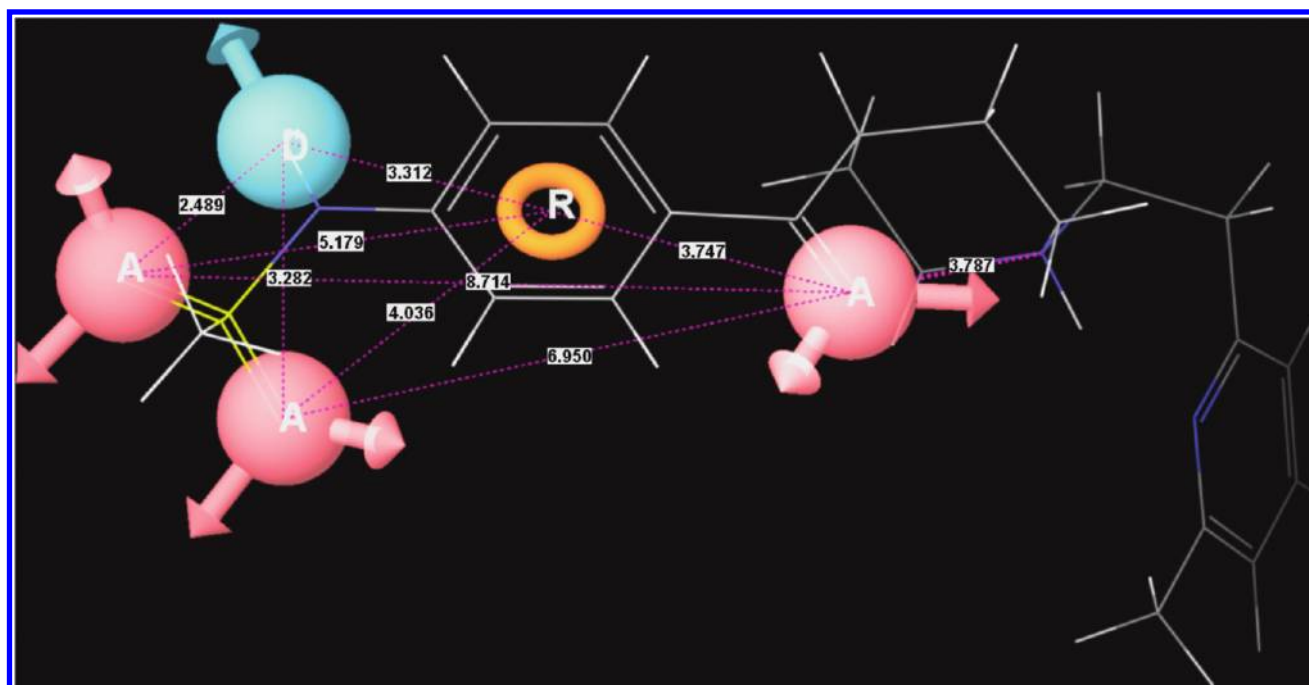the molecules leading to the disruption the adjacent aromatic ring interactions with the central cavity residues at the hERG.[43] Although there are many high-affinity hERG blockers possessing methylsulfonylanilide terminal group in literature, to limit a bias toward the methylsulfonylanilide unit, the number of methylsulfonamide compounds in the training set at Table 1 was limited to 3 which they have observed pIC$_{50}$ values between 7.49 and 8.14 and relatively large diversity in structures.

Most of the known potassium channel blockers are thought to primarily target a pocket located in the IC cavity of the channel.[19,22] One distinct feature of hERGs compared to other potassium channels, is replacement of the aliphatic side-chains in the distal S6 helix (Ile or Val in many voltage-gated channels) by aromatic residues (i.e., Y652 and F656; see Supporting Information for the sequence alignment of the S6 helix of the hERG1 and Kv1.2 ion channels, Figure S5).[44]

Inhibitory potencies of hERG1 blockers, measured with traditional patch-clamp electrophysiology, vary from low nanomolar binding affinities (e.g., sertindole and dofetilide) to μM range (e.g., KN-93 and Grepafloxacin). Extensive alanine scanning mutagenesis of the S6 helix has been used to characterize the binding specificity of several drugs.[45] Both Y652 and F656 have been reported as a predicament for the high-affinity block. Other residues (i.e., T623 and S624) located at the apex of the pore helix are thought to be involved in drug binding underlying the pocket's specificity.

The derived AAADR.7 model covers the whole structure— activity profile for the used data set subsequently merged with the receptor-based homology model of hERG1[30] (Supporting Information Figure S1). Our main objective for merging the ligand-based virtual homology model and the receptor-based atomistic model is to examine the fitness of these two models (i.e., in terms of chemical interactions of critical amino acids for blocking affinity at the inner cavity of the hERG pore domain model with pharmacophore interactions derived by the ligand-based model).

In Supporting Information Figure S1, the AAADR.7 pharmacophore model is shown with vector features (i.e., red and blue vectors show hydrogen-bond acceptor (labeled as A) and hydrogen-bond donor (labeled as D), respectively, whereas aromatic ring features is labeled as R). The *vector* feature refers to any pharmacophore property with directionality. The pharmacophore feature term here is used to describe the characteristic of a chemical structure that may facilitate a noncovalent interaction between a ligand and a biological target. While it is very tempting to explain properties of the pharmacophore model in terms of a "better" or "worse" fits to detailed atomistic representation of the receptor and the vector features of the model, it may include some limitations. The main challenge relating magnitudes of the given vector feature from the model with the docked conformation from atomistic modeling is an apparent ligand conformational dynamics. Flexible molecules such as dofetilide can undergo large structural fluctuations (e.g., 3—4 Å), while bound to the hERG1 cavity. Most of the blockers are large and flexible molecules that can make multiple contacts with IC-cavity of the hERG1 and thus a distance to the protein residue should be seen as a statistical quantity only.

Combining inputs from receptor modeling, in silico alanine scanning and QSAR pharmacophore analysis makes it possible to provide some general principles underlying the high-affinity block. For example, a tyrosine side-chain of Y652 is located in the region of the S6 that may form favorable interactions with the **A** pharmacophore. This stabilizing interaction involves cation-π interactions between the π-electron system in the aromatic ring of Y652 and the partially or fully positively charged functional groups (e.g., tertiary amines) is common in many K-channels blockers. The $\pi-\pi$ interactions between phenyl rings in the channel and a blocker is likely to be important as well. The $\pi-\pi$ interactions of Y652 with aromatic ring pharmacophore (labeled as **R** in Supporting Information Figure S1) are part of an optimal pharmacophore. This finding is consistent with several experimental studies concluding that aromatic properties of Y652 play

an important role in the binding interactions of high affinity blockers).[46,47]

On the basis of the atomistic receptor model, F656, Y652, and A653 at the inner cavity of hERG1 form hydrophobic interactions with ligands for the blocking potency. In addition, T623, S624, L622 and A653 amino acid residues form hydrogen bonds with blockers at the IC cavity of hERG1 (L622 and A653 may form hydrogen bonds from backbone chains). The developed pharmacophore-model shows that Y652 is the critical amino acid for hydrophobic interactions with ligands, whereas Y616, T623, S624, S649, Y652, and F656 amino acids form hydrogen bonds with ligands at the IC cavity (F656 may form hydrogen bonds from the backbone).

Therefore, analysis of the receptor-based and ligand-based modeling suggest that ideal high-affinity hERG1 blocker has to be developed under following constraints: (i) matching hydrophobic group must form close contacts with Y652 and F656, (ii) presence of the hydrogen-bond acceptor pharmacophores capable of interactions with the T623 side chains, and (iii) hydrogen-bond donor pharmacophores close to the S624.

We made an effort to develop such an ideal blocker using general pharmacophore approach. The AAADR.7 general pharmacophore model possesses three pharmacophore sites: one hydrogen-bond accepting, one donating and an aromatic ring pharmacophores. Distances between these pharmacophores are shown in Figure 4. On the basis of the constructed model, chemical moieties of an ideal hERG blocker should fit with these corresponding pharmacophores. All active compounds used in the training set match well with topologies of these five pharmacophores. Although there have been several ligand-based models presented in the literature, two crucial elements, namely, a basic center and lipophilicity, are commonly reported as key determinants in hERG blockers.[19−23] In our model, an aromatic ring surrounded by hydrogen-bond accepting (minimum and maximum distances between aromatic ring and hydrogen-bond accepting pharmacophores are measured as 3.7 and 5.2 Å) and hydrogen-bond donor (distance between aromatic ring and hydrogen-bond donating pharmacophore is measured as 3.3 Å) pharmacophores are essential elements for high affinity hERG blocking. An amine group positioned close (2.7−3.8 Å) to one of the hydrogen-bond accepting pharmacophores (A4) was seen in all active ligands used for construction of the training set (Figure 4). This basic center underlies some polarity in the central cavity; thus, it may lower penalty for replacement of the potassium ion bound to IC site. The ideal distance (based on reference ligand alignment; in this study potent and selective hERG blocker E4031 (compound 12 in Table 1) was selected as reference compound) between the nitrogen atom of the amine group and the center of the aromatic ring is measured as 6.3 Å.

The resulting ideal blocker should have the following characteristics determined from a combination of 3D QSAR and molecular docking studies: (1) an aromatic ring should be surrounded by three hydrogen-bond acceptors and a hydrogen-bond donor group and (2) a basic center (i.e., an amine or an amidine group) should be located around 6.3 Å from the aromatic ring. Top docking poses at the S6 inner helix showed that the center of the inner cavity is filled by the basic center of the blocker. (Figure 3)

CONCLUSIONS

By using in vitro IC_{50} data of hERG inhibitors, we built a pharmacophore model that contains all of the characteristics of

the structure−activity relationships that were revealed to be essential for their activity. The best model (AAADR.7) that showed high r^2 and q^2 coefficients, as well as low probability and standard deviations, was selected from 44 constructed models. This pharmacophore was used to construct a 3D-QSAR model that predicts pIC_{50} values of blockers with an unknown hERG1 inhibitory activity. The derived ligand-based model was merged with a receptor-based model and a high consistency between these models was found. Importantly, the analysis of the constructed model has shown that it can serve as a tool to scan and predict hERG inhibition of candidate drugs before their synthesis. The constructed model is expected to differentiate between weak and strong hERG blockers. The AAADR.7 model and its associated pharmacophore are available upon request.

ASSOCIATED CONTENT

ⓢ Supporting Information. Scoring functions of PHASE, tables showing 3D-QDAR results and external test set compounds, and figures showing essential amino acids, experimental binding energies, top docking poses, change in hERG IC_{50} with modification of methylsulfonamide groups, and sequence alignment of S6. This material is available free of charge via the Internet at http://pubs.acs.org.

AUTHOR INFORMATION

Corresponding Author
*E-mail: snoskov@ucalcary.ca (SYN.); hduff@ucalgary.ca (HJD).

ACKNOWLEDGMENT

REFERENCES

(1) Curran, M. E.; Splawski, I.; Timothy, K. W.; Vincent, G. M.; Green, E. D.; Keating, M. T. A Molecular Basis for Cardiac-Arrhythmia—Herg Mutations Cause Long Qt Syndrome. *Cell* **1995**, *80*, 795–803.

(2) Tseng, G. N. I(Kr): The hERG Channel. *J. Mol. Cell. Cardiol.* **2001**, *33*, 835–49.

(3) Vandenberg, J. I.; Walker, B. D.; Campbell, T. J. HERG K+ Channels: Friend and Foe. *Trends. Pharm. Sci.* **2001**, *22*, 240–246.

(4) Splawski, I.; Shen, J. X.; Timothy, K. W.; Lehmann, M. H.; Priori, S.; Robinson, J. L.; Moss, A. J.; Schwartz, P. J.; Towbin, J. A.; Vincent, G. M.; Keating, M. T. Spectrum of Mutations in Long-QT Syndrome Genes KVLQT1, HERG, SCN5A, KCNE1, and KCNE2. *Circulation* **2000**, *102*, 1178–1185.

(5) Witchel, H. J.; Hancox, J. C. Familial and Acquired Long QT Syndrome and the Cardiac Rapid Delayed Rectifier Potassium Current. *Clin. Exp. Pharmacol. Physiol.* **2000**, *27*, 753–766.

(6) Huang, F. D.; Chen, J.; Lin, M.; Keating, M. T.; Sanguinetti, M. C. Long-QT Syndrome-Associated Missense Mutations in the Pore Helix of the HERG Potassium Channel. *Circulation* **2001**, *104*, 1071–1075.

472

dx.doi.org/10.1021/ci100409y |*J. Chem. Inf. Model.* 2011, 51, 463–474

(7) Lees-Miller, J. P.; Duan, Y. J.; Teng, G. Q.; Thorstad, K.; Duff, H. J. Novel Gain-of-Function Mechanism in K$^+$ Channel-Related Long-QT Syndrome: Altered Gating and Selectivity in the HERG1 N629D Mutant. *Circ. Res.* **2000**, *86*, 507–513.

(8) Teng, G. Q.; Lees-Miller, J. P.; Duan, Y. J.; Li, B. T.; Li, P.; Duff, H. J. [K$^+$](o)-Dependent Change in Conformation of the HERG1 Long QT Mutation N629D Channel Results in Partial Reversal of the In Vitro Disease Phenotype. *Cardiovasc. Res.* **2003**, *57*, 642–650.

(9) Sanguinetti, M. C.; Mitcheson, J. S. Predicting Drug—hERG Channel Interactions that Cause Acquired Long QT Syndrome. *Trends Pharm. Sci.* **2005**, *26*, 119–124.

(10) Petko, C.; Bradley, D. J.; Tristani-Firouzi, M.; Cohen, M. I.; Sanatani, S.; Saarel, E. V.; Albaro, C. A.; Etheridge, S. P. Congenital Long QT Syndrome in Children Identified by Family Screening. *Am. J. Cardiol.* **2008**, *101*, 1756–1758.

(11) Nattel, S.; Carlsson, L. Innovative Approaches to Anti-arrhythmic Drug Therapy. *Nat. Rev. Drug Discovery* **2006**, *5*, 1034–1049.

(12) Sanguinetti, M. C.; Mitcheson, J. S. Predicting Drug-hERG Channel Interactions that Cause Acquired Long QT Syndrome. *Trends Pharmacol. Sci.* **2005**, *26*, 119–124.

(13) Mitcheson, J.; Perry, M.; Stansfeld, P.; Sanguinetti, M. C.; Witchel, H.; Hancox, J. Structural Determinants for High-affinity Block of hERG Potassium Channels. *Novartis Found. Symp.* **2005**, *266*, 136–150 Discussion 150−158.

(14) Lees-Miller, J. P.; Duan, Y. J.; Teng, G. Q.; Duff, H. J. Molecular Determinant of High-Affinity Dofetilide Binding to HERG1 Expressed in Xenopus Oocytes: Involvement of S6 Sites. *Mol. Pharmacol.* **2000**, *57*, 367–374.

(15) Du, L. P.; Li, M. Y.; You, Q. D. Interactions between hERG Potassium Channel and Blockers. *Curr. Top. Med. Chem.* **2009**, *9*, 330–338.

(16) Sanguinetti, M. C.; Tristani-Firouzi, M. hERG Potassium Channels and Cardiac Arrhythmia. *Nature* **2006**, *440*, 463–469.

(17) Stork, D.; Timin, E. N.; Berjukow, S.; Huber, C.; Hohaus, A.; Auer, M.; Hering, S. State Dependent Dissociation of HERG Channel Inhibitors. *Br. J. Pharmacol.* **2007**, *151*, 1368–1376.

(18) Yang, Q.; Du, L. P.; Tsai, K. C.; Wang, X. J.; Li, M. Y.; You, Q. D. Pharmacophore Mapping for Kv1.5 Potassium Channel Blockers. *QSAR Comb. Sci.* **2009**, *28*, 59–71.

(19) Cavalli, A.; Poluzzi, E.; De Ponti, F.; Recanatini, M. Toward a Pharmacophore for Drugs Inducing the Long QT Syndrome: Insights from a CoMFA Study of HERG K$^+$ Channel Blockers. *J. Med. Chem.* **2002**, *45*, 3844–3853.

(20) Pearlstein, R. A.; Vaz, R. J.; Kang, J. S.; Chen, X. L.; Preobrazhenskaya, M.; Shchekotikhin, A. E.; Korolev, A. M.; Lysenkova, L. N.; Miroshnikova, O. V.; Hendrix, J.; Rampe, D. Characterization of HERG Potassium Channel Inhibition using CoMSiA 3D QSAR and Homology Modeling Approaches. *Bioorg. Med. Chem. Lett.* **2003**, *13*, 1829–1835.

(21) Dearden, J. C.; Netzeva, T. I. QSAR Modelling of hERG Potassium Channel Inhibition with Low-Dimensional Descriptors. *J. Pharm. Pharmacol.* **2004**, *56*, S82–S82.

(22) Recanatini, M.; Poluzzi, E.; Masetti, M.; Cavalli, A.; De Ponti, F. QT Prolongation through hERG K$^+$ Channel Blockade: Current Knowledge and Strategies for the Early Prediction During Drug Development. *Med. Res. Rev.* **2005**, *25*, 133–166.

(23) Thai, K. M.; Ecker, G. F. Binary QSAR Model for Classification of hERG Potassium Channel Blockers. *Bioorg. Med. Chem.* **2008**, *16*, 4107–4119.

(24) Osterberg, F.; Aqvist, J. Exploring Blocker Binding to a Homology Model of the Open hERG K$^+$ Channel using Docking and Molecular Dynamics Methods. *FEBS Lett.* **2005**, *579*, 2939–2944.

(25) Stary, A.; Wacker, S. J.; Boukharta, L.; Zachariae, U.; Karimi-Nejad, Y.; Aqvist, J.; Vriend, G.; de Groot, B. L. Toward a Consensus Model of the hERG Potassium Channel. *ChemMedChem* **2010**, *5*, 455–467.

(26) Stansfeld, P. J.; Gedeck, P.; Gosling, M.; Cox, B.; Mitcheson, J. S.; Sutcliffe, M. J. Drug Block of the hERG Potassium Channel: Insight from Modeling. *Proteins: Struct., Funct., Bioinf.* **2007**, *68*, 568–580.

(27) Kamiya, K.; Niwa, R.; Mitcheson, J. S.; Sanguinetti, M. C. Molecular Determinants of hERG Channel Block. *Mol. Pharmacol.* **2006**, *69*, 1709–1716.

(28) Recanatini, M.; Cavalli, A.; Masetti, M. Modeling HERG and Its Interactions with Drugs: Recent Advances in Light of Current Potassium Channel Simulations. *ChemMedChem* **2008**, *3*, 523–535.

(29) Fernandez, D.; Piper, D.; Tristani-Firouzi, M.; Sanguinetti, M. C. HERG Channel Gating and Block. *J. Mol. Cell. Cardiol.* **2005**, *39*, 168–169.

(30) Lees-Miller, J. P.; Subbotina, J. O.; Guo, J.; Yarov-Yarovoy, V.; Noskov, S. Y.; Duff, H. J. Interactions of H562 in the S5 helix with T618 and S621 in the Pore Helix are Important Determinants of hERG1 Potassium Channel Structure and Function. *Biophys. J.* **2009**, *96*, 3600–3610.

(31) Dixon, S. L.; Smondyrev, A. M.; Knoll, E. H.; Rao, S. N.; Shaw, D. E.; Friesner, R. A. PHASE: A New Engine for Pharmacophore Perception, 3D QSAR Model Development, and 3D Database Screening: 1. Methodology and Preliminary Results. *J. Comput.-Aided Mol. Des.* **2006**, *20*, 647–671.

(32) *Maestro*, version 8.5.207; *LigPrep*, version 2.2; Schrodinger. LLC: Portland, OR, 2007.

(33) Friesner, R. A.; Murphy, R. B.; Repasky, M. P.; Frye, L. L.; Greenwood, J. R.; Halgren, T. A.; Sanschagrin, P. C.; Mainz, D. T. Extra Precision Glide: Docking and Scoring Incorporating a Model of Hydrophobic Enclosure for Protein−Ligand Complexes. *J. Med. Chem.* **2006**, *49*, 6177–6196.

(34) Jones, G.; Willett, P.; Glen, R. C.; Leach, A. R.; Taylor, R. Development and Validation of a Genetic Algorithm for Flexible Docking. *J. Mol. Biol.* **1997**, *267*, 727–748.

(35) Bohm, H. J. The Development of a Simple Empirical Scoring Function to Estimate the Binding Constant for a Protein−Ligand Complex of Known Three-Dimensional Structure. *J. Comput.-Aided Mol. Des.* **1994**, *8*, 243–256.

(36) Sherman, W.; Day, T.; Jacobson, M. P.; Friesner, R. A.; Farid, R. Novel Procedure for Modeling Ligand/Receptor Induced Fit Effects. *J. Med. Chem.* **2006**, *49*, 534–553.

(37) Wolber, G.; Langer, T. LigandScout: 3D Pharmacophores Derived from Protein-Bound Ligands and Their use as Virtual Screening Filters. *J. Chem. Inf. Model* **2005**, *45*, 160–169.

(38) Leong, M. K. A Novel Approach using Pharmacophore Ensemble/Support Vector Machine (PhE/SVM) for Prediction of hERG Liability. *Chem. Res. Toxicol.* **2007**, *20*, 217–226.

(39) Subbotina, J.; Yarov-Yarovoy, V.; Lees-Miller, J.; Durdagi, S.; Guo, J.; Duff, H. J.; Noskov, S. Y. Structural Refinement of the hERG1 Pore and Voltage-Sensing Domains with ROSETTA-Membrane and Molecular Dynamics Simulations. *Proteins: Struct., Funct., Bioinf.* **2010**, *78*, 2922–2934.

(40) Ekins, S.; Crumb, W. J.; Sarazan, R. D.; Wikel, J. H.; Wrighton, S. A. Three-Dimensional Quantitative Structure−Activity Relationship for Inhibition of Human Ether-a-go-go-Related Gene Potassium Channel. *J. Pharmacol. Exp. Ther.* **2002**, *301*, 427–434.

(41) Kubinyi, H. Comparative Molecular Field Analysis (CoMFA). In *The Encyclopedia of Computational Chemistry*; John Wiley & Sons: Chichester, U.K., 1998; pp 448−460.

(42) Holtje, H. D.; Sippl, W.; Rognan, D.; Folkers, G. *Molecular Modeling: Basic Principles and Applications*, 3rd ed.; Wiley-VCH: NJ, 2008; Chapter 2, pp 32−49.

(43) Jamieson, C.; Moir, E. M.; Rankovic, Z.; Wishart, G. Medicinal Chemistry of hERG Optimizations: Highlights and Hang-Ups. *J. Med. Chem.* **2006**, *49*, 5029–5046.

(44) Mitcheson, J. S.; Chen, J.; Lin, M.; Culberson, C.; Sanguinetti, M. C. A Structural Basis for Drug-Induced Long QT Syndrome. *Proc. Natl. Acad. Sci. U.S.A.* **2000**, *97*, 12329–12333.

(45) Chen, J.; Seebohm, G.; Sanguinetti, M. C. Position of Aromatic Residues in the S6 Domain, Not Inactivation, Dictates Cisapride

473

dx.doi.org/10.1021/ci100409y |*J. Chem. Inf. Model.* 2011, 51, 463–474

Sensitivity of HERG and eag Potassium Channels. *Proc. Natl. Acad. Sci. U.S.A.* **2002**, *99*, 12461–12466.

(46) Choe, H.; Nah, K. H.; Lee, S. N.; Lee, H. S.; Jo, S. H.; Leem, C. H.; Jang, Y. J. A Novel Hypothesis for the Binding Mode of HERG Channel Blockers. *Biochem. Biophys. Res. Commun.* **2006**, *344*, 72–78.

(47) Dalibalta, S.; Mitcheson, J. S. Antitargets: Methods and Principles in Medicinal Chemistry *hERG Channel Physiology and Drug-Binding Structure−Activity Relationships*; Wiley-VCH: Weinheim, Germany, 2008; Chapter 4, pp 89−108.